# CHAPTER IV
# RESULTS AND DISCUSSION

This chapter discusses about the effects of temperature and residence time on the pyrolysis of waste tires, and also the effects of bifunctional catalysts prepared by the incipient wetness impregnation of noble metal (Ru) on the zeolites (HMOR and HZSM5).

## 4.1 Effect of Pyrolysis Conditions

The conditions in pyrolysis played the most important role to the pyrolysis product distribution. In 1998, Cunliffe studied the pyrolysis of waste tire in static bed reactor and found that the final pyrolysis temperature had an influence on product distribution. As the final temperature increased, the yields to liquid fraction decreased whereas the yields to gas fraction was increased. Dai *et al.* (2000) used a circulating fluidized bed reactor to pyrolyzed the waste tire. The effects of temperature, residence time, and heating rate were studied. They found that high temperature and long residence time yielded more light hydrocarbon gases such as $CH_4$, $C_2H_2$ and $H_2$, and less heavy hydrocarbon gases.

### 4.1.1 Effect of Temperature on Pyrolysis Product

The pyrolysis process was carried out in a bench-scale autoclave reactor which the temperature was varied from 400 to 700°C with the heating rate of 10°C/min from room temperature to a final temperature at the atmospheric pressure. The reaction was maintained for 90 minutes after the final pyrolysis temperature was reached. Three main products obtained from pyrolysis of waste tire were solid residue, pyrolysis oil and pyrolysis gas.

#### *4.1.1.1 Percentage of Product Yields*

The yields of pyrolysis products obtained at different temperatures and residence time are reported as the gas-to-liquid ratio as shown in Figure 4.1.

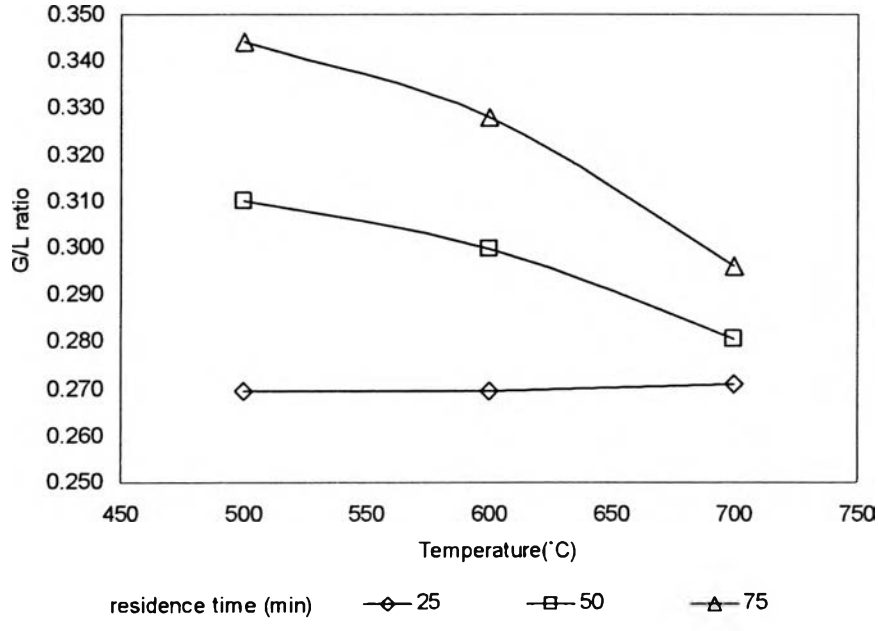


**Figure 4.1** G/L ratio at various residence time.

At the lower residence time, the gas-to-liquid ratio (G/L) is unaffected by temperature. However, it gradually decreases with temperature at higher residence time, meaning that the amount of gas decreases with temperatures at a fixed residence time. For the effects of residence time, the longer residence time produced higher amount of lower molecular weight product. Hence, the G/L ratio is increased at high residence time. The yield to solid fraction decreases with temperature, reaching value around 46% for all conditions, except for the case of 400°C and 50 min residence time, at which a part of polymer in tire does not decompose, remaining in the solid residue. So, the conversion at this condition is lower than another case. The solid fraction is basically constant for pyrolysis at different temperatures. Cunliffe and Williams (1998) suggested that the yields to solid fraction in temperature ranging from 400-700°C were very fluctuate, and depended on the operating conditions such as, heating rate, particle size, and residence time. They obtained the constant yields around 38% when the temperature was varied from 450 up to 600°C. Similar to Kawacami *et al.*(1980) for tire pyrolysis at temperature ranging from 540 to 750°C in a rotative reactor, they received the

yields between 38 to 40 wt. % with a heating rate of 30°C/min. In some cases, the increase in solid yields at high pyrolysis temperature was observed, this can be suggested to be due to the carbonaceous deposits occur during aromatization reaction. The raw data are shown in Appendix B.

*4.1.1.2 Gas Compositions*

The results of the yields by weight and volume of the different gas fractions obtained from gas chromatrography analysis at various pyrolysis temperatures and residence time showed that main gases were methane, ethane, mixed-C4 and other hydrocarbon gases. Cypres and Bettens (1989) have suggested that light hydrocarbons are derived from secondary aromatization reactions. Similarly, Williams and Taylor (1990) have reported that methane and ethylene are formed from secondary aromatizations, which are the reaction to produce aromatic hydrocarbons. Kaminsky *et al.*(1980) also showed that the gas fraction consisted of $H_2$, CO, $CO_2$ and hydrocarbons such as $CH_4$,$C_2H_6$, $C_2H_4$, $C_3H_8$, $C_3H_6$, $C_4H_{10}$, $C_4H_8$ and $C_4H_6$. The results in this experiment are shown in Table 4.1 and Figure 4.2.

**Table 4.1** Gas composition at various temperatures

| gas composition | Temperature (°C) | | | | | | | |
|---|---|---|---|---|---|---|---|---|
| | 400 | | 500 | | 600 | | 700 | |
| | wt.% | vol.% | wt.% | vol.% | wt.% | vol.% | wt.% | vol.% |
| Methane | 11.46 | 27.77 | 19.20 | 39.37 | 21.00 | 41.04 | 23.96 | 46.13 |
| Ethylene | 5.92 | 8.20 | 8.94 | 10.48 | 11.37 | 12.70 | 10.38 | 11.43 |
| Ethane | 13.62 | 17.60 | 15.86 | 17.35 | 15.72 | 16.39 | 13.57 | 13.94 |
| Propylene | 7.88 | 7.28 | 9.89 | 7.73 | 11.56 | 8.61 | 10.51 | 7.71 |
| Propane | 9.01 | 7.94 | 8.08 | 6.03 | 6.95 | 4.94 | 5.80 | 4.07 |
| mixed-C4 | 30.91 | 20.67 | 21.09 | 11.93 | 20.70 | 11.17 | 19.25 | 10.23 |
| mixed-C5 | 12.19 | 6.57 | 10.30 | 4.70 | 8.24 | 3.58 | 9.70 | 4.15 |
| mixed-C6 | 7.87 | 3.55 | 5.22 | 1.99 | 3.64 | 1.32 | 5.38 | 1.93 |
| mixed-C7 | 0.53 | 0.21 | 0.72 | 0.24 | 0.38 | 0.12 | 0.65 | 0.20 |
| mixed-C8 | 0.60 | 0.21 | 0.68 | 0.20 | 0.46 | 0.13 | 0.81 | 0.22 |

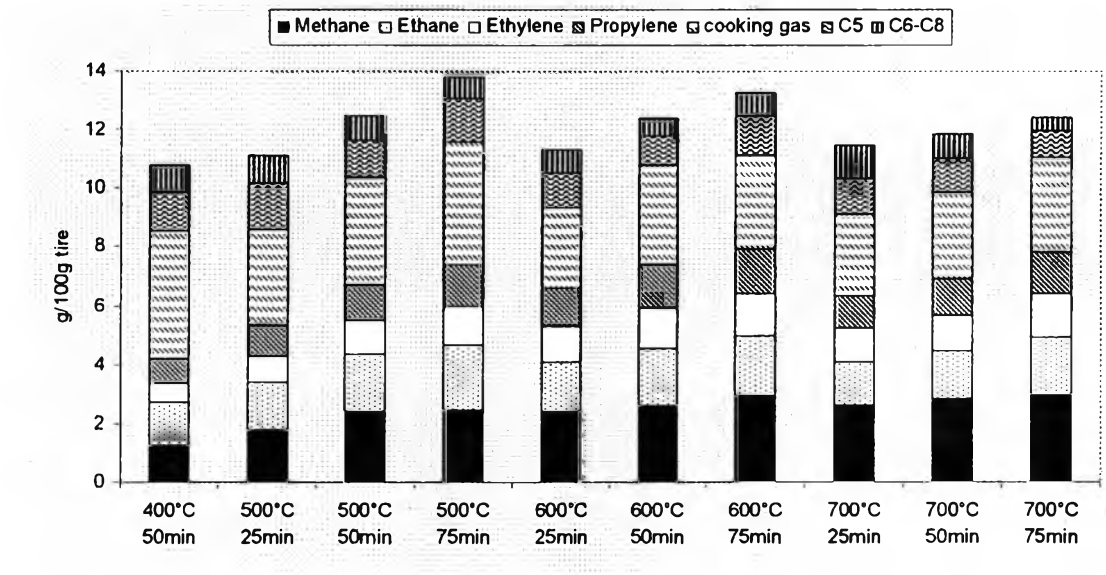


**Figure 4.2** Gas productions at different temperatures.

As can be seen from Table 4.1 and Figure 4.2, the main compositions of gaseous fraction are hydrocarbon gases such as methane, ethane, ethylene, propylene, and mixed $C_4$-$C_8$. The yields to gaseous product are increased with increasing residence time at a fixed temperature. The increase of gas yield as residence time increases is mainly due to the increase of light hydrocarbon gases such as, methane, ethane, ethylene, propylene, and also the cooking gas which is hereby defined as the mixture of propane and mixed-$C_4$. Many authors agreed that light hydrocarbons were formed from the cracking molecules of SBR, the main composition of tire, which also form the shorter aliphatic hydrocarbon chains (Laresgoiti *et al.*, 2000; Cypres *et al.*, 1989).

The detail of the influence of pyrolysis temperature on the gaseous composition can be observed in Figures 4.3–4.5. At longest residence time, the yields of light hydrocarbon molecules such as methane, ethylene and propylene are increased with temperature whereas the amount of heavy molecules such as mixed-$C_5$, mixed-$C_6$, and mixed-$C_7$ are decreased. At the lower residence time, the formation of light hydrocarbon molecules such as, ethane, ethylene, propane and propylene reached the maximum at 600°C whereas the mixed-$C_5$ and mixed-$C_6$ went to minimum. At the final pyrolysis temperature at 400°C, the main composition is

mixed-$C_4$. This can be explained by the insufficient heat for completely cracking the whole raw material. At the temperatures higher than 500°C up to 700°C, the main compositions are light hydrocarbons molecules such methane, ethane, ethylene and propylene. These light hydrocarbon molecules are formed by the secondary cracking reaction which are favored at high temperature. As the pyrolysis temperature increases, the yields to propane decrease, consequently leading to the increase in methane yields. The results are similar to Li *et al.*(2006). They studied catalytic pyrolysis of $C_4$ and found that, as the temperature went up from 450 to 650°C, the yields to methane and ethane increased whereas the yields to propane decreased. For every case, the amount of heavy hydrocarbon gases such as mixed-$C_7$ and mixed-$C_8$ can be observed in only a trace amount because most of heavy molecules were trapped and condensed in the condenser before being passed through the gas collecting bag. The details for each composition are shown in Appendix E.

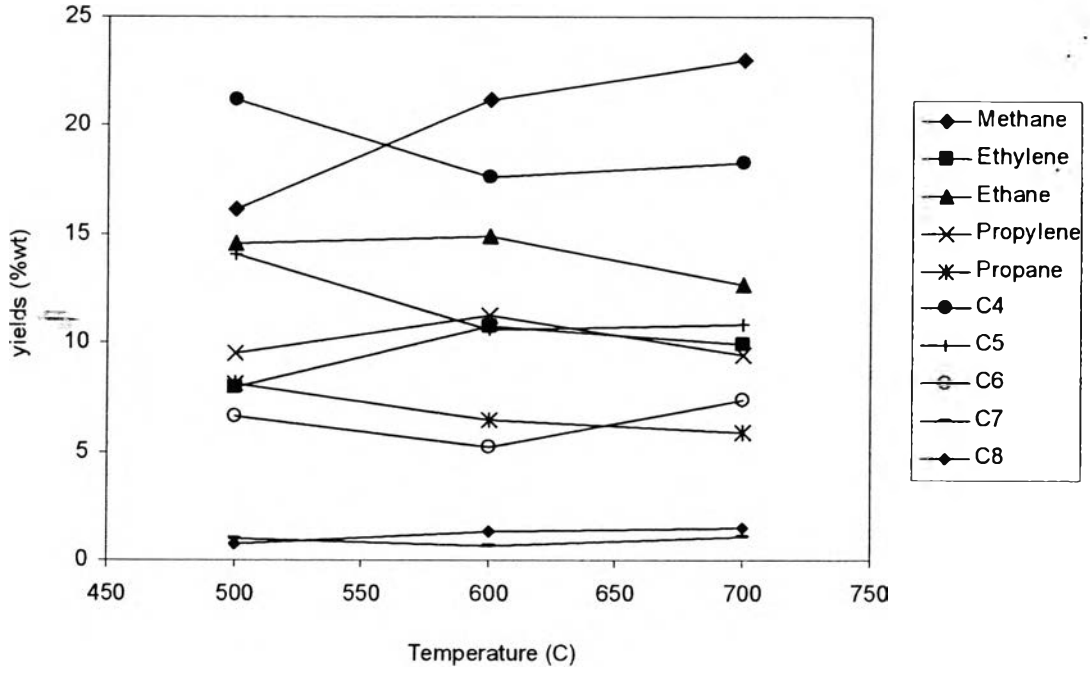


**Figure 4.3** Effect of temperature on the gas compositions at 25 min residence time.

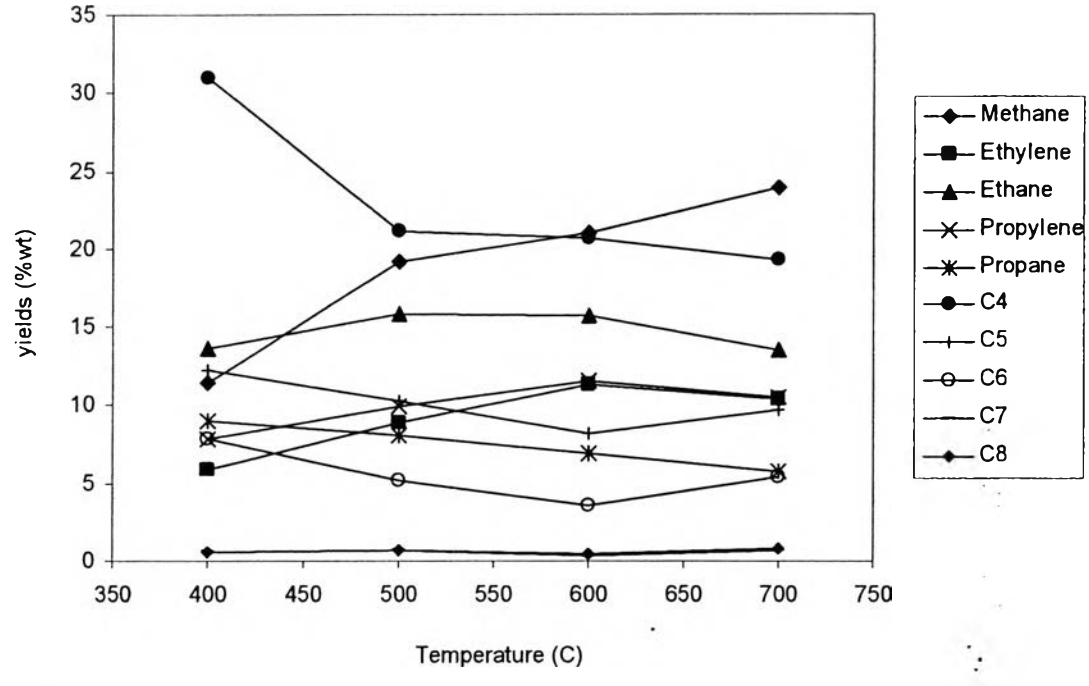


**Figure 4.4** Effect of temperature on the gas compositions at 50 min residence time.

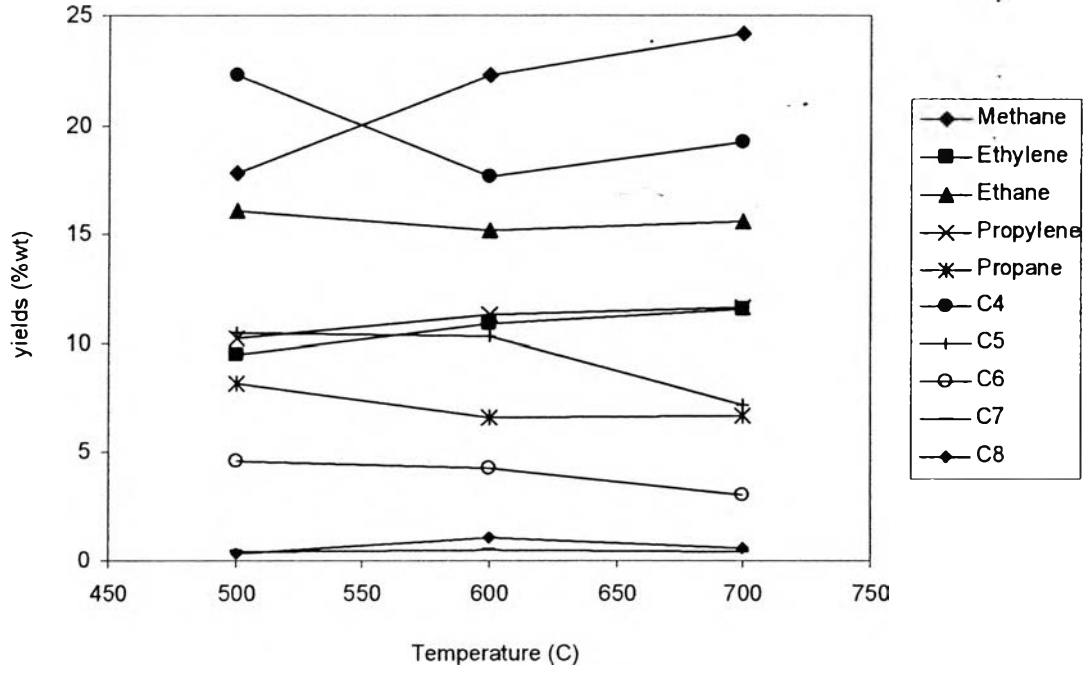


**Figure 4.5** Effect of temperature on the gas compositions at 75 min residence time.

*4.1.1.3 Heating Value of Gases*

Figure 4.6 shows the heating value of the gas obtained from the pyrolysis of waste tire at different temperatures for each residence time. The gas-heating value is expressed in kJ ($kgmole^{-1}$) of gas. The curve for 25 and 50 min residence time increases up to an approximately constant value attained at the highest temperature. The increase is sharper at the initial step, and is constant at high temperatures. The approximately constant value at high temperature can be described by elevation of gas compositions which yields difference heating value. The longer residence time can produce the highest heating value. This can be explained by the increase of combustible component gases as the temperature and residence time increases.

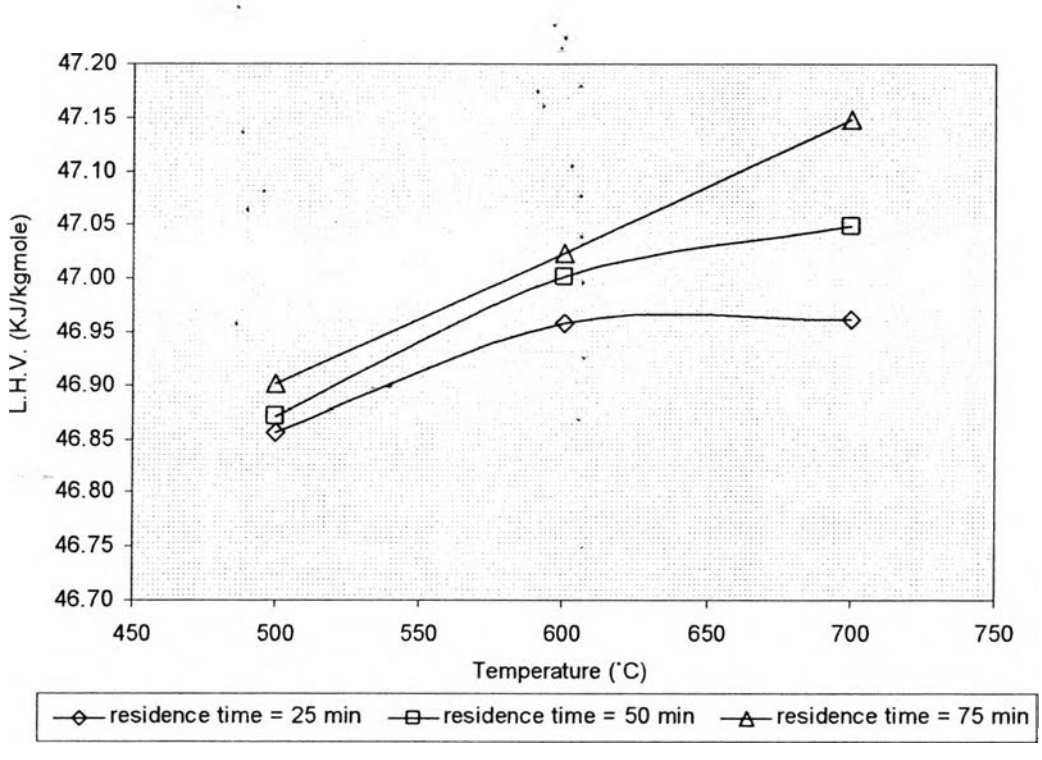


**Figure 4.6** Gas-heating values at different temperatures and residence time.

4.1.2 Effect of Residence Time

The residence time is one the most important parameters affecting to the pyrolysis process. Dai *et al.* (2001) studied the effect of residence time on the pyrolysis of waste tire in fluidized-bed reactor. They found that the yields to char and oil decreased while the yields to gas increased when the residence time increased.

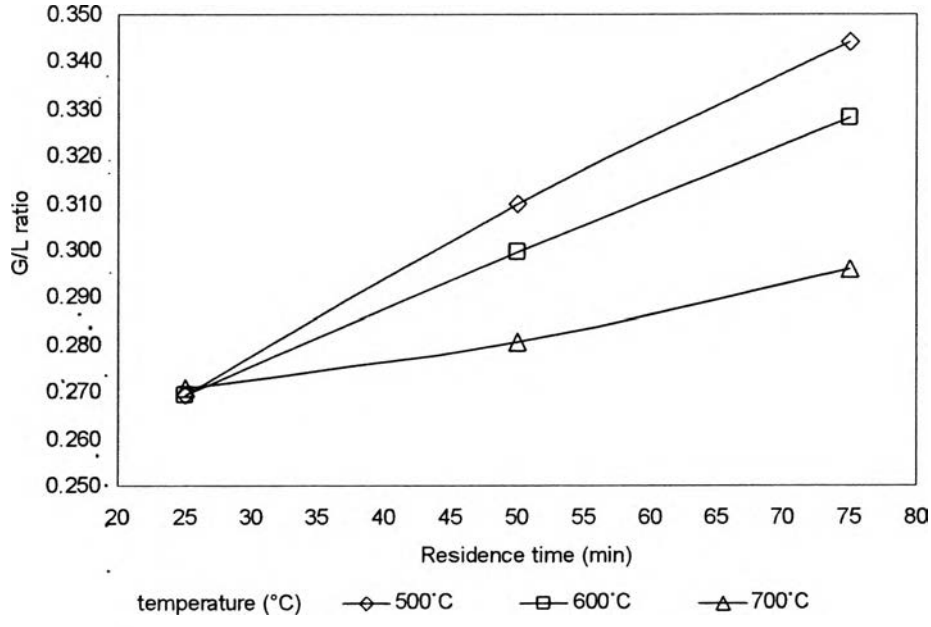


**Figure 4.7** G/L ratio at various temperatures.

From Figure 4.7, the effects of residence time are greater than the effects of pyrolysis temperature. As can be seen from G/L ratio of pyrolysis products, at lowest pyrolysis temperature, the G/L ratio is increased with residence time whereas it is decreased with increasing temperature. All cases show the same trend in increasing liquid yield when the residence time is decreased. The increases in liquid yield can be described by the suppression of secondary reactions by decreasing the time for the product to stay in the reactor. Similar to Cypres and Bettens (1989), the rate of removal of pyrolysis product from the reactor was increased by increasing the flow rate of nitrogen carrier gas, and it was found that the yield of liquid increased from 34.4% to 41.6% because of the reduction in the secondary reactions. For the gas

fraction, the increases in residence time increased the yield of gaseous products. This can be easily described by the increment of time for cracking reaction to occur. The longer residence time promoted the secondary cracking reactions to convert higher molecular weight products to lower molecules, or it allows small fractions of molecules to recombine, resulting in new and bigger molecules.

The effect of residence time on gas compositions can be observed in Figures 4.8-4.10. The main trend is that the light hydrocarbon gases from methane up to mixed-C4 increased, and heavier hydrocarbons are decreased with the increase of residence time. This effect can be more obviously seen at high pyrolysis temperatures, which favor the secondary reactions. The secondary reaction is occurring to convert the primary product into more stable, less reactive alternatives. The secondary reaction that can occurred in pyrolysis process are tar cracking reaction, shift reaction, oligomerization, cyclization, H-transfer reaction and aromatization (Aguado *et al*, 1999). For pyrolysis at high temperature, the secondary reaction that possibly occurred are char reaction, tar cracking, shift reaction, etc. (Dia *et al*, 2001), more than at low temperature. Moreover, the yields to light olefins such as, ethylene and propylene are slightly decreased, and the yield to methane is increased when the pyrolysis temperature is increased at fixed residence time. This observation is similar to Lovett *et al.* (1997) and Sodero *et al.* (1995), who studied the pyrolysis of waste plastic to produce light gases. They found that at a fixed residence time, the yield to propylene decreased resulting in an increase in the yields to ethylene and methane as the temperature increased.

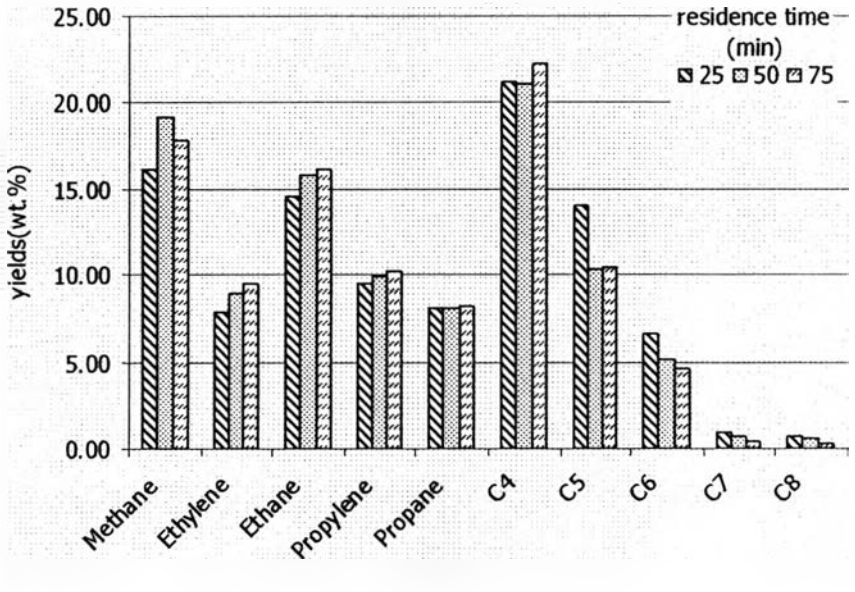


**Figure 4.8** Gas composition obtained from pyrolysis reaction at 500°C.

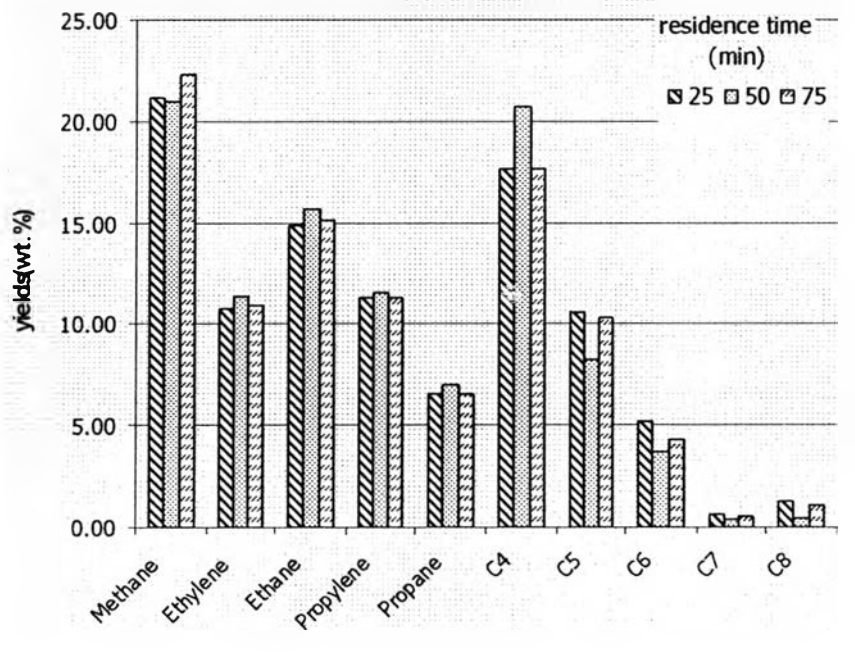


**Figure 4.9** Gas composition obtained from pyrolysis reaction at 600°C.

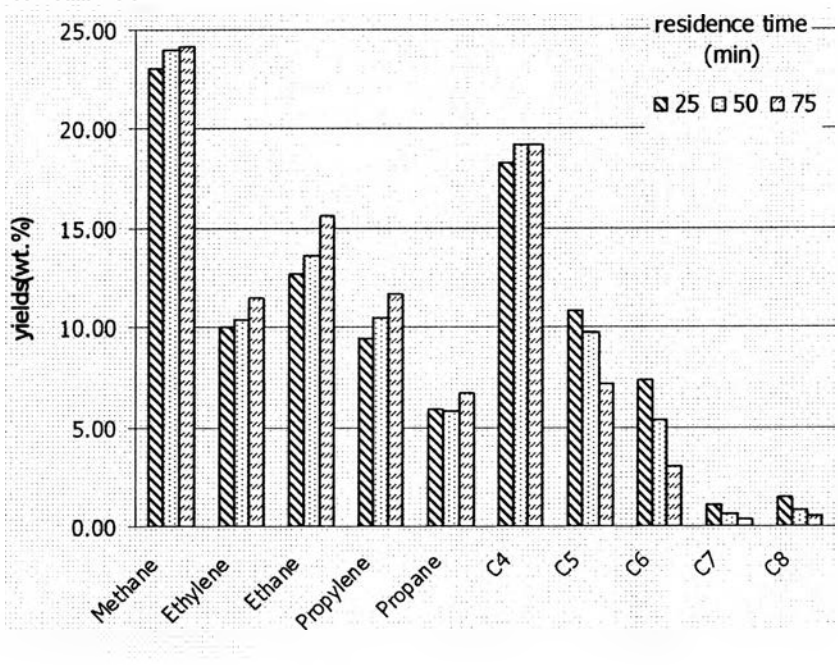


**Figure 4.10** Gas composition obtained from pyrolysis reaction at 700°C.

4.1.3 Light Olefins Production

Light olefins are very useful starting materials for chemical industry. It is well known that the most important commercial light olefins production process is stream thermal cracking that uses light oils or light hydrocarbons as a feedstock. However, light olefins production has been studied by many researchers via many types of reaction such as stream cracking, catalytic cracking and pyrolysis reactions. In this research, pyrolysis gas, which is not condensed, in the glass condensers will pass through the gas sampling bag. Then, the collected gas was injected to gas-chromatography in order to determine the weight percentage of the gaseous composition. The gaseous product can be classified into two main fractions; n-paraffins and light olefins. In this research, the light olefin products were focused on ethylene and propylene only. The results for light olefins production per kilogram of waste tire are shown in Figure 4.11.

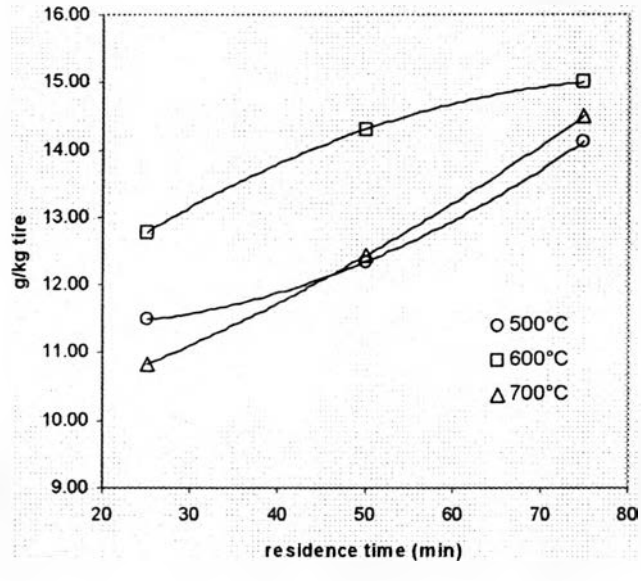


(a)

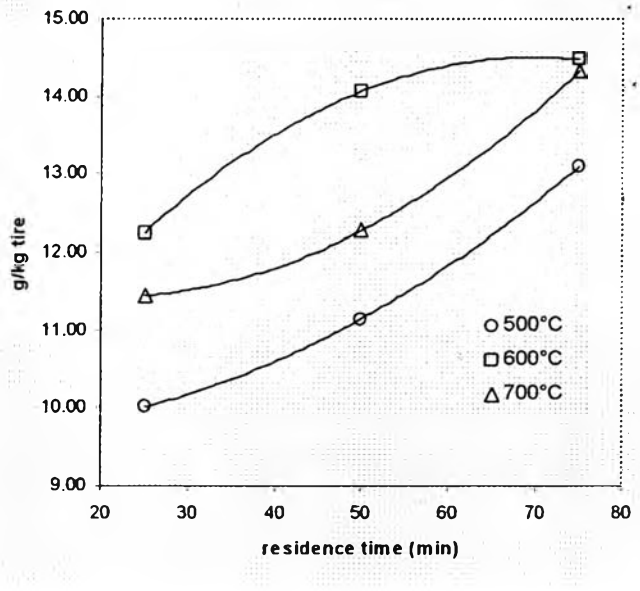


(b)

**Figure 4.11** Light olefins production at different residence time and temperatures: Ethylene, and (b) Propylene.

From Figure 4.11, selectivity to both light olefins increases as the residence time increases. But for the effects of temperature, 600°C seems to be the

best operating condition for ethylene and propylene production because it gave the highest selectivity of the two products. At 500°C, the production of light olefins does not reach the maximum due to the insufficient energy to convert higher molecules such as mixed-$C_4$ and mixed-$C_5$ to ethylene and propylene. The major product at high temperature is methane. This can be described by the conversion of hydrocarbon molecules such as ethane, propane and mixed-$C_5$ by the cracking reaction. Moreover, the yields to unsaturated hydrocarbon gases (ethylene and propylene) exceed the yields to saturated hydrocarbons (ethane and propane) when the pyrolysis temperature is increased. The same result was found by Lee *et al.* (1995) and Dai *et al.* (2000). They suggested that saturated hydrocarbons were decomposed to unsaturated hydrocarbon gases as the temperature increased. It is also possible that more unsaturated hydrocarbon gases are derived directly from thermal decomposition of polymers making up the tire, since the rubber used in tire manufacture are characterized by carbon-carbon double bonds within the rubber molecule (Dodds *et al.*, 1983).

The results of light olefins production can be clearly observed by the ratio of light olefins to paraffins as shown in Table 4.2. Although 600°C is the best condition for light olefin production, but the ratio of olefins to paraffins is lower than at the highest pyrolysis temperature and the longest residence time. This can be suggested that some of large molecules such as cooking gas cannot be cracked at 600°C, so that the paraffin amount was still high as compared with pyrolysis at 700°C. This can also be confirmed by the percentage of ethylene, propylene and total light olefins as a function of pyrolysis temperature as shown in Figure 4.12.

**Table 4.2** The ratio of light olefins to paraffin

| Residence time (min) / Temperature (°C) | 25 | 50 | 75 |
|---|---|---|---|
| **500** | 0.212 | 0.232 | 0.246 |
| **600** | 0.283 | 0.297 | 0.286 |
| **700** | 0.241 | 0.264 | 0.302 |

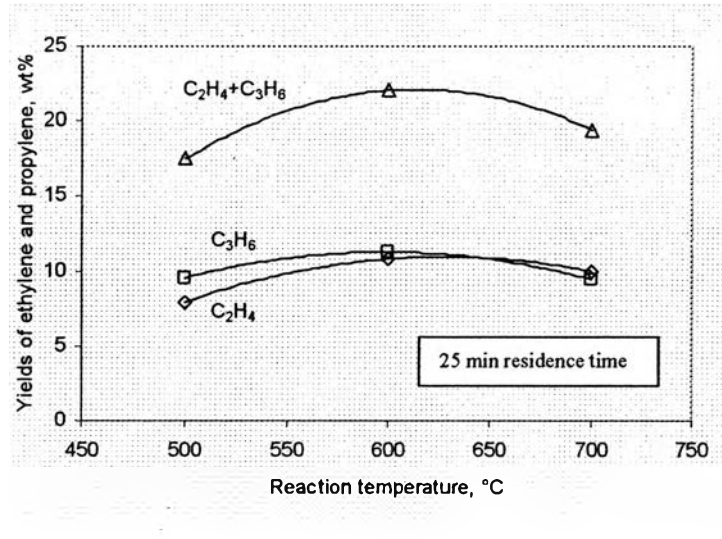


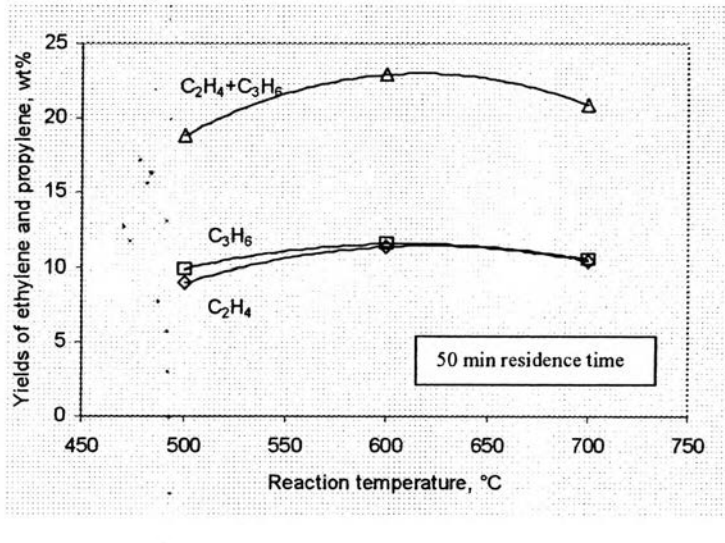


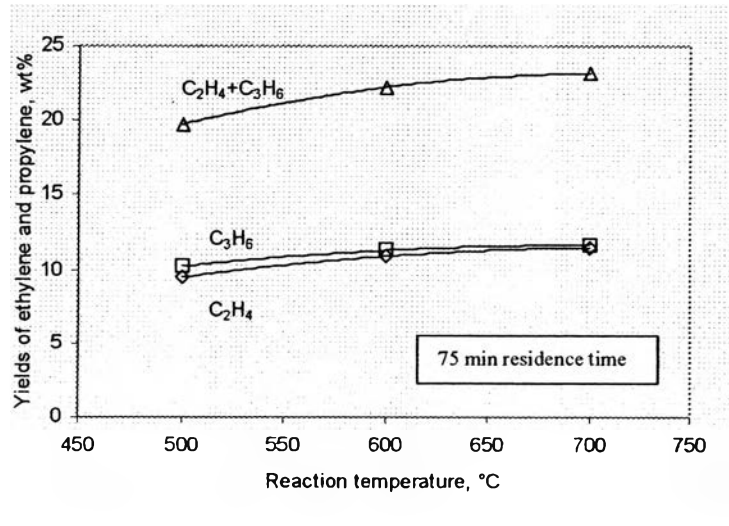


**Figure 4.12** Effect of pyrolysis temperature on the yield of ethylene and propylene.

4.1.4 Liquid Analysis

Liquid products obtained from the waste tire pyrolysis process, which are usually termed oils, can be classified into petroleum fractions by the boiling point and carbon cut ranges of hydrocarbons from SIMDIST-GC analysis as shown in Table 4.3.

**Table 4.3** The boiling point and carbon ranges of refinery products (Speight, 2002)

| Fraction | Carbon range | Boiling point (°C) |
|---|---|---|
| Gasoline | $C_5$-$C_9$ | 15.5-149 |
| Kerosene | $C_{10}$-$C_{13}$ | 149-232 |
| Gas oil | $C_{14}$-$C_{20}$ | 232-343 |
| Light vacuum gas oil | $C_{21}$-$C_{23}$ | 343-371 |
| Heavy vacuum gas oil | $C_{24}$-$C_{50}$ | 371-566 |

*4.1.4.1 Petroleum Fraction Analysis*

From Figures 4.13-4.15, the main fractions of maltene from the pyrolysis of waste tire are gasoline, kerosene, gas oil, light vacuum gas oil and heavy vacuum gas oil. The gasoline and kerosene fractions tend to decrease at high pyrolysis temperatures and long residence time whereas the yields to light vacuum gas oil and heavy vacuum gas oil fractions are increased. The yield to gas oil fraction is comparable for all cases. These can be described by the cracking of the chain of heavy molecules such as gasoline and kerosene to lighter products whereas the vacuum gas oil could be formed from the recombination of the cracked molecules of gasoline and kerosene. Similar results were reported by Meng *et al.* (2006).

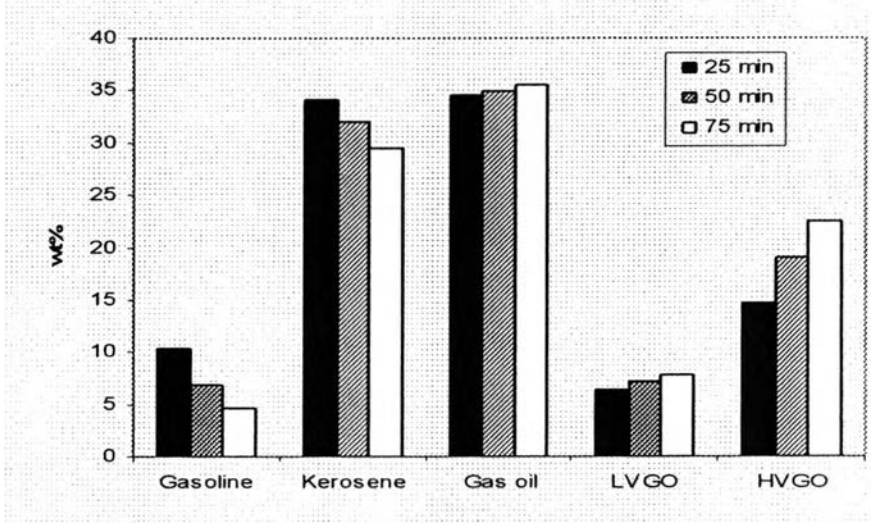


**Figure 4.13** Petroleum fractions in maltenes obtained from different residence time at the temperature of 500°C.

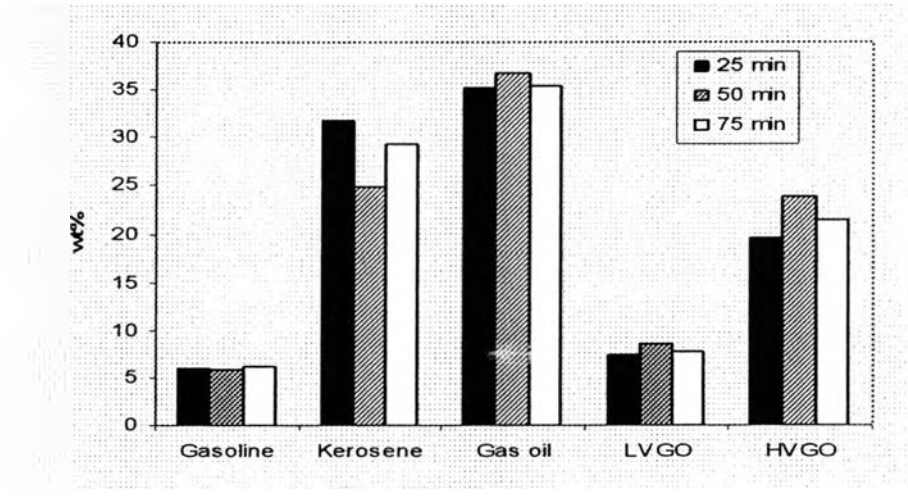


**Figure 4.14** Petroleum fractions in maltenes obtained from different residence time at the temperature of 600°C.

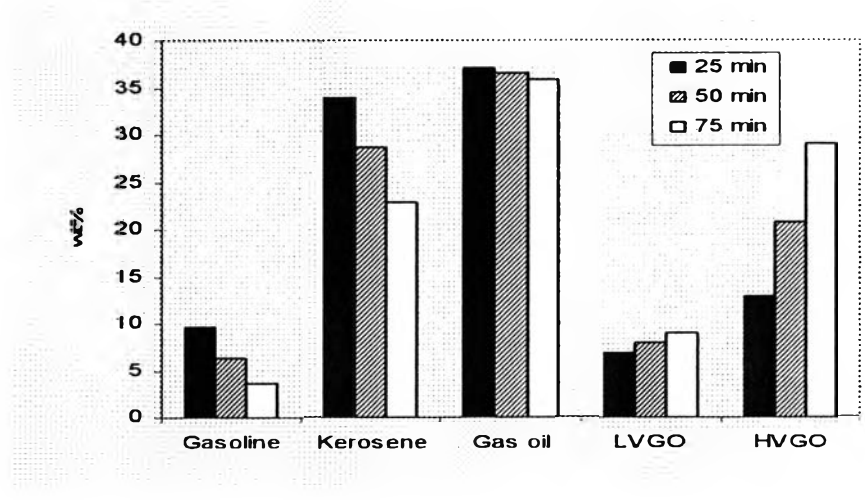


**Figure 4.15** Petroleum fractions in maltenes obtained from different residence time at the temperature of 700°C.

Moreover, the quality of liquid products can be roughly estimated from the carbon number distribution of maltenes as shown in Figure 4.16. From the figure, the carbon number distributions of maltenes for pyrolysis at the lowest temperature are dominated in the kerosene and gas oil ranges. When the temperature increases at the lowest residence time, the yields to gasoline and kerosene fractions are decreased. When the residence time is prolonged, the yield to heavy fraction is increased whereas the yields to lighter fractions are decreased.

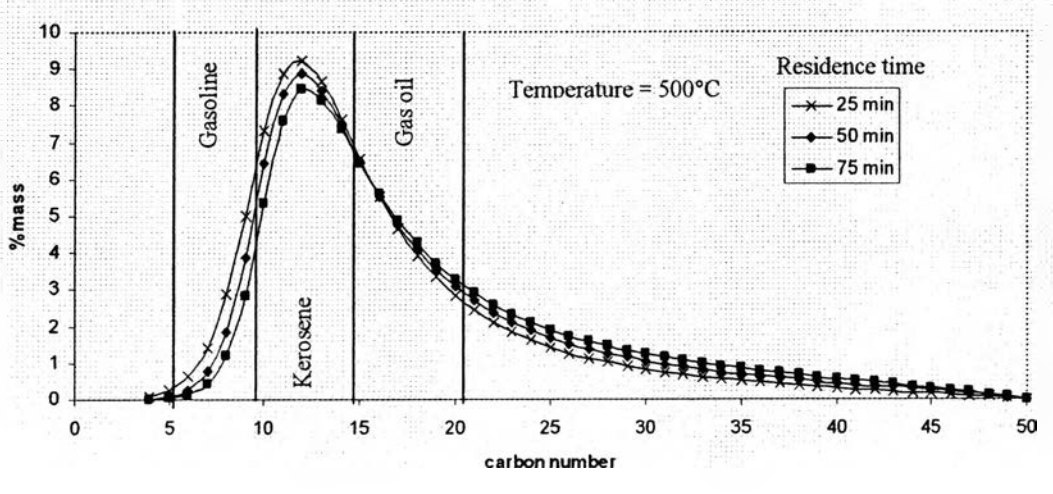

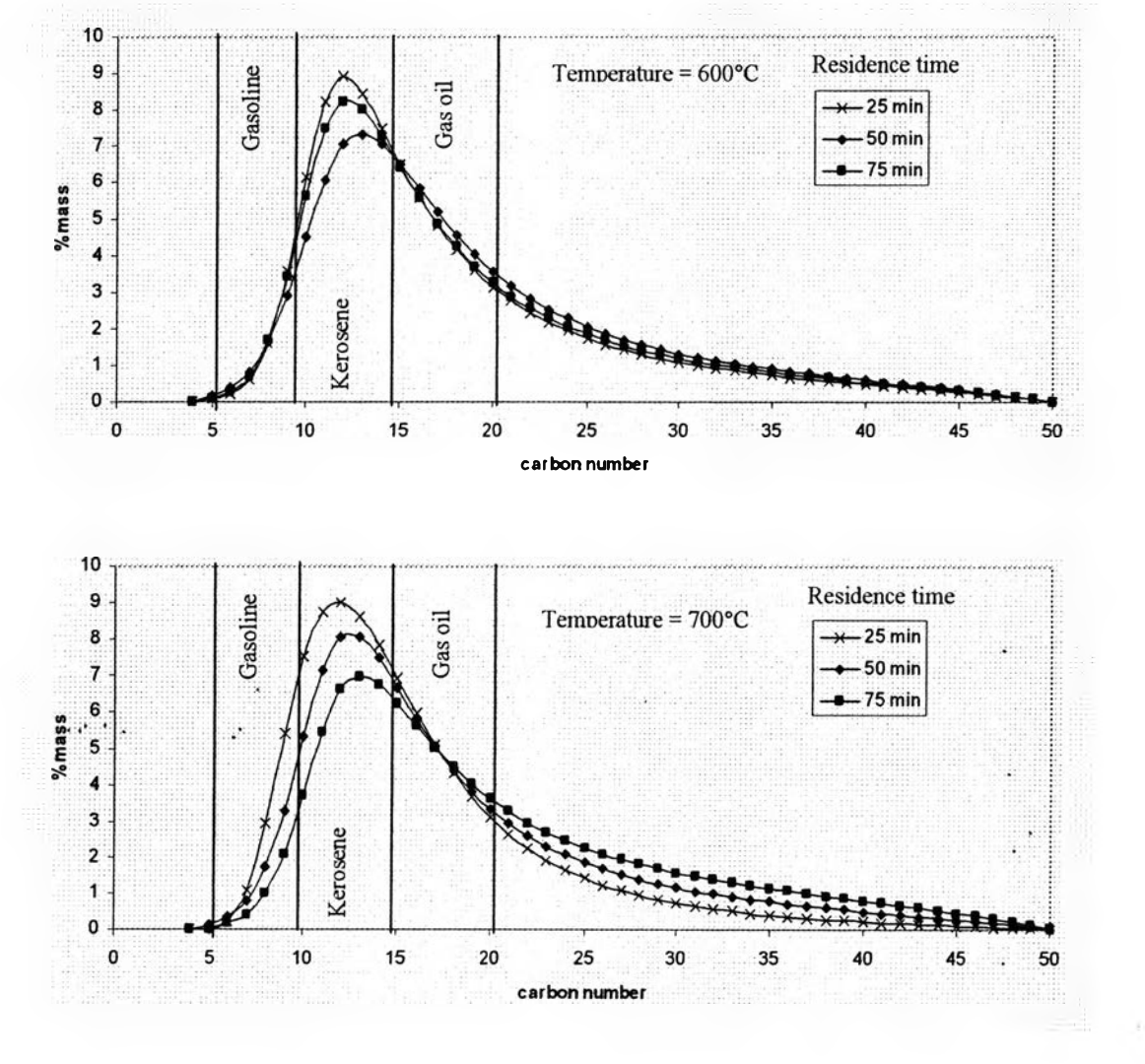


**Figure 4.16** Carbon number distribution of maltenes obtained from different temperatures and residence time.

*4.1.4.2 Quality of Pyrolysis Oil*

After the pyrolytic oil was mixed with n-pentane, the asphaltene was precipitated out from the solution. The results show that pyrolysis temperature has an effect to the amount of asphaltene to maltene ratio. At the lowest temperature, the amount of asphaltene formation is about 0.2%, and increases to 0.35% when the temperature increases to 600°C at an average residence time. The lowest amount of asphaltene formation is observed at the highest temperature. Residence time also the major effects to the amount of asphaltene. Prolonging the

residence time results in a high amount of asphaltene. This effect can be easily seen from pyrolysis at 700°C. At lowest residence time, the asphaltene formation is 0.08% and increases to 0.18 and 0.27% when the residence time is increased to 50 and 75 minute, respectively. And, it is possible that at 700°C, the polyaromatic molecules might be cracked to lighter molecules, resulting in the decrease in the amount of asphaltene at this temperature.

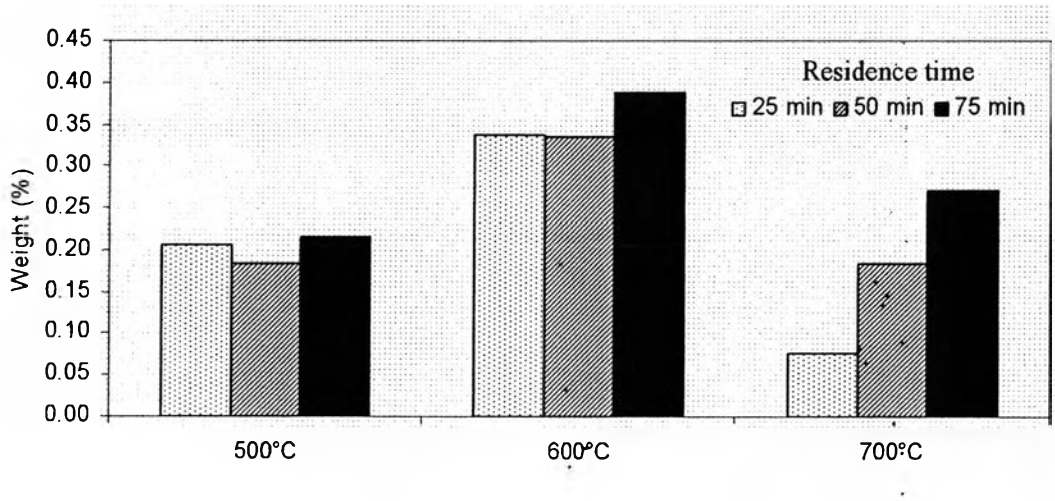


**Figure 4.17** Weight percentage of asphaltene in pyrolytic oils at difference residence time and temperatures.

After that, the maltenes were separated into fractions according to the chemical composition such as saturated hydrocarbons, mono-aromatics, di-aromatics, poly-aromatics and polar-aromatics by using liquid adsorption chromatography. Figure 4.18 shows that the ratio of saturated hydrocarbons for pyrolysis at 500°C and 75 min residence time is the highest. This can be explained by the optimum thermal cracking efficiency at an optimum temperature and residence time. Moreover, the ratio of saturated hydrocarbons to total aromatic hydrocarbons is lower at higher pyrolysis temperature, meaning that more aromatic hydrocarbons are formed at high temperatures. Similar trends have been reported by Cypres and Bettens (1989), Wolfson *et al.* (1969) and Kaminsky and Sinn (1980).

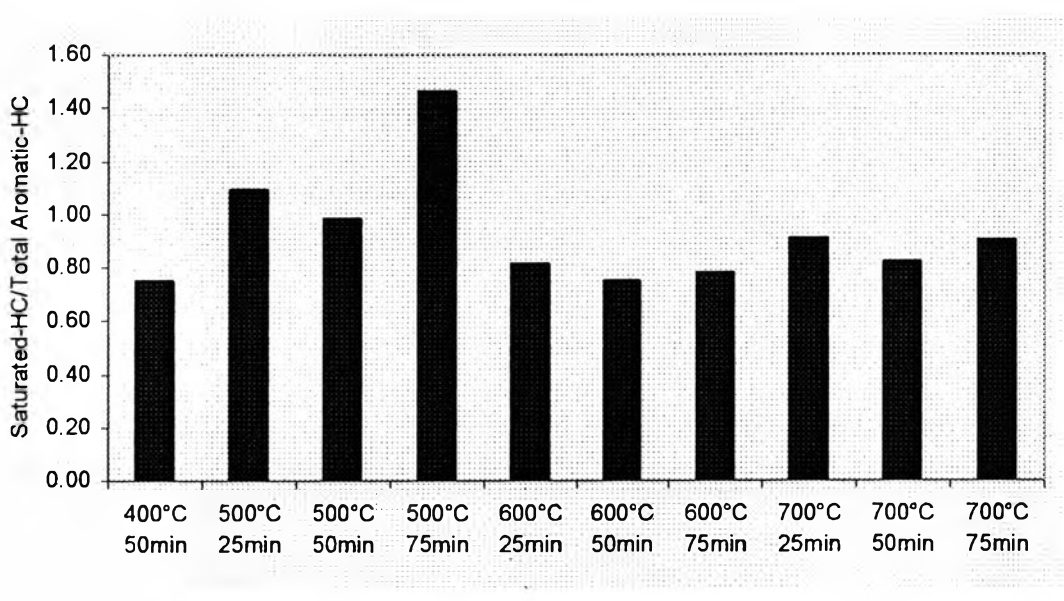


**Figure 4.18** The ratio of saturated hydrocarbons to total aromatic hydrocarbons in maltenes obtained from various temperatures and residence time.

Moreover, the details of chemical compositions in pyrolysis oil have been investigated. Due to some concern in the presence of poly-aromatic hydrocarbons (PAHs) in the environment, since PAHs comprise of the largest group of carcinogenic compounds. The PAHs found in tyre pyrolysis oil consist largely of alkylated naphthalenes, fluorenes and phenanthrenes. The details of PAH formation in pyrolysis of waste tire are reported in Table 4.4. From the table, the amount of poly-aromatic hydrocarbons in oil increase as the pyrolysis temperature increases at a fixed residence time. At high temperatures, PAHs formation reach maximum at 50 min residence time, then decrease at 75 min residence time. This can be suggested that PAHs formation might be decreased when the residence time is prolonged at a very high temperature.

Poly-aromatic hydrocarbons in pyrolysis of waste tire have also been reported by many authors. Cunliffe *et al.* (1998) studied on the composition of oil from the batch pyrolysis of waste tire. They found that the total PAHs content in oils increased from 1.53 wt.% at 450°C to 3.43 wt.% of total oil at 600°C. Cypres and Bettens (1989) pyrolyzed scrap tires by two-stage process. They

found that the concentration of PAHs increased with increasing post-cracking temperature. Wolfson *et al.* (1969) pyrolyzed scrap tire in a retort heated to 500°C and separated the oil into light and heavy fractions. They found that the heavy oil fraction contained a large amount of the PAHs, biphenyl, acenaphthene and alkyl naphthalenes.

The increase in PAHs with increasing of pyrolysis temperature has also been reported by other researchers. Williams and Taylor (1993) studied the pyrolysis of waste tire in a batch reactor with the post-pyrolysis heating of the tire vapors. They found that the concentration of PAHs in oil increased from 1.4 wt.% at 500°C post-pyrolysis temperature to more than 10 wt.% at 720°C post-pyrolysis temperature. Cypres and Bettens (1989), also using the post-pyrolysis reactor, found that the increase of PAHs in oil was from the secondary reactions of vapors. A Diels-Alder reaction mechanism has been suggested for the increase in aromatic content with increasing temperature. The pyrolysis of waste tire leads to the formation of ethylene, propylene and butadiene, which can react to form cyclic alkenes. The dehydrogenation of cyclic alkene compounds with six carbon atoms occurs to produce single ring aromatic compounds, and as a result the subsequent associative reactions lead to the formation of PAHs, such as naphthalene and phenanthrene.

**Table 4.4** Poly-aromatic hydrocarbon formation, wt% of maltene

| Residence time (min) / Temperature (°C) | 25 | 50 | 75 |
|---|---|---|---|
| **500** | 5.87 | 6.75 | 9.55 |
| **600** | 8.19 | 14.49 | 11.44 |
| **700** | 10.97 | 17.87 | 14.57 |

Further confirmation that secondary reactions of hydrocarbons at moderate to high temperatures can produce PAHs has been shown in the studies on pure hydrocarbon compounds by Cypres *et al.* (1987). They pyrolyzed the *n*-decane to produce alkene by the thermal degradation and post-cracking of alkenes

between 600 and 900°C with 2 sec residence time. The light olefins were decreased, and consequently the formation of single ring aromatic compounds, such as benzene, toluene and alkyl-aromatics was increased by Diels-Alder reactions. They concluded that aromatic hydrocarbons were formed at a very high temperature (>700°C) with a short contact time or at a low temperature with increasing contact time by Diels-Alder reactions between the two species of light olefins formed by cracking of paraffins. The formation of PAHs via the Diels–Alder reaction scheme is illustrated in Fig. 4.19.

In addition, it has been shown that the increase in the residence time of pyrolysis vapor in the hot zone of the reactor will lead to the increase in secondary reactions such as the formation of PAHs (Williams and Taylor., 1993).

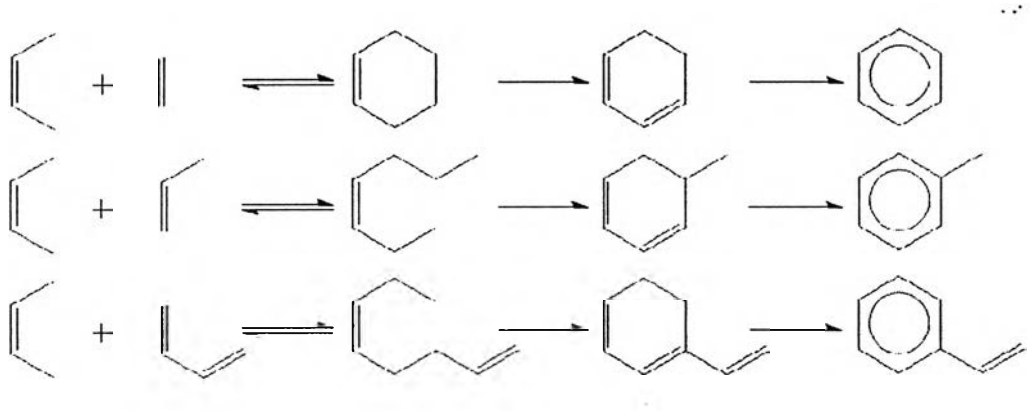

**Figure 4.19** Aromatic and alkylaromatic formation by Diels-Alder reaction. (Cypres *et al.*, 1987)

## 4.2 Effect of Catalyst Supports

The zeolites selected for using as a catalyst support in this research have the structure and properties as shown in Table 4.5. All of the zeolites were loaded with 1.0% ruthenium metal to be used as bifunctional catalysts.

**Table 4.5** Zeolite properties (Roldan *et al.*, 2005)

| Zeolite | Dimension | Membered ring (MR) | Si/Al | Surface area ($m^2/g$) | Pore size (Å) |
|---|---|---|---|---|---|
| MOR | 1D | 12 | 38 | ~ 380 | 6.5 x 7.0 |
| ZSM5 | 3D | 10 | 23 | ~ 360 | 5.4 x 5.6 |

### 4.2.1 Product Distributions

The effects of different bifunctional catalysts are shown in Figure 4.20. The yield to gaseous fraction increases about 2 times, and consequently decreases the liquid fraction with using bifunctional catalysts as compared to non-catalytic case. This can be described by the high cracking activity of bifunctional catalysts that heavy hydrocarbon molecules were cracked resulting in a high amount of light hydrocarbon molecules in the gaseous fraction. For the solid fraction, Ru/ZSM5 produces a higher amount of solid residue than Ru/MOR. This is possible that ZSM5 has higher surface activity than MOR, so that it can produce a high amount of aromatic hydrocarbon molecule which can deposite on the solid residue resulting in the increase of solid yields.

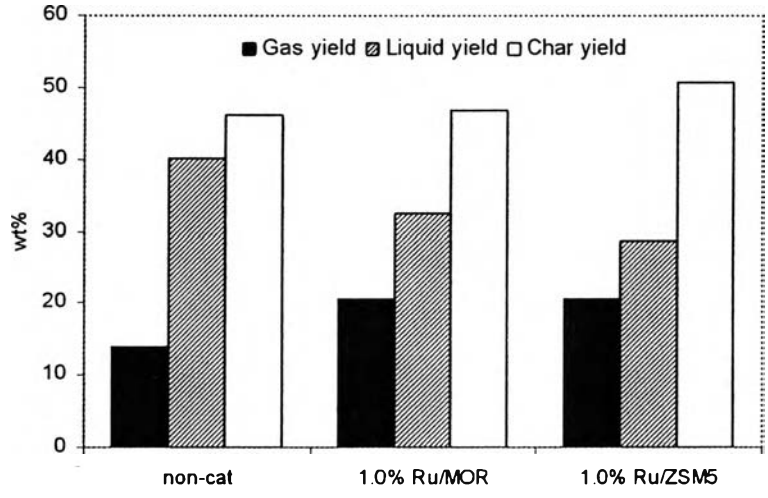


**Figure 4.20** Product distributions for different catalysts.

4.2.2 Gas Compositions

The compositions of pyrolysis gas obtained from pyrolysis with the bifunctional catalysts are similar to non-catalytic case. From Figure 4.21, the catalysts have higher selectivity to propane whereas they have lower the selectivity to ethylene and propylene than non-catalytic pyrolysis. Moreover, Ru/ZSM5 can produce the highest amount of propane and the lowest amount of light olefins.

In 2005, Bortnovsky *et al.* studied the cracking of pentene to light olefins by using different zeolites. They found that ZSM5 with low Si/Al ratio have a high conversion of pentene but low selectivity to light olefins, and has a high yield of undesirable products such as paraffins and aromatic hydrocarbons. So for this case, it might be possible that the molecules of $C_4$-$C_5$ were cracked to form propane molecule over the bifunctional catalysts. And it is also possible that ruthenium metal hydrogenated light olefin molecules resulting in a high amount of $C_2$ and $C_3$ paraffins.

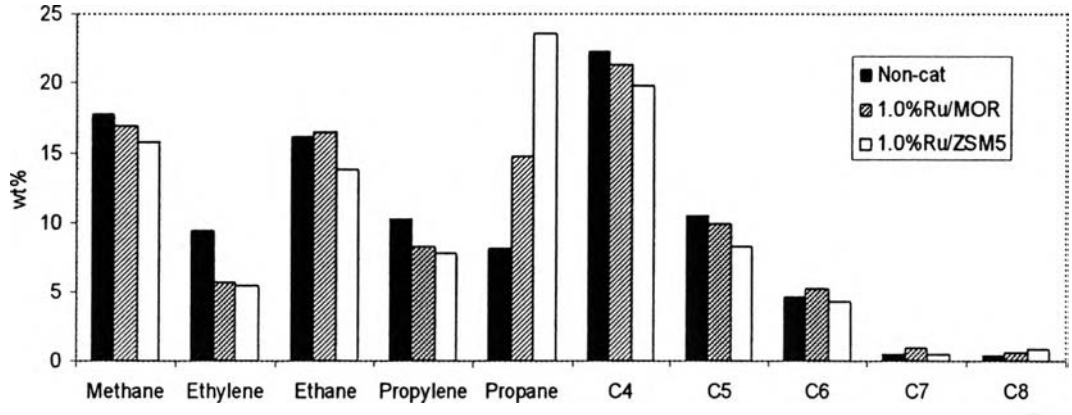


**Figure 4.21** Gas compositions obtained from different catalysts.

4.2.3 Light Olefins Production

Figure 4.22 shows the production of light olefins with different bifunctional catalysts. The yields to total light olefins are comparable for non-catalytic and catalytic pyrolysis with Ru/ZSM5. This can be suggested that Ru/MOR can enhance the production of light olefins. Similarly, Bortnovsky *et al.* (2005) reported that mono-dimensional zeolites such as, mordenite and ZSM12 with a high concentration of acid site had high activity and selectivity to $C_2$-$C_4$ olefins. The reaction was suggested to proceed via the formation of oligomeric carbenium ion intermediates.

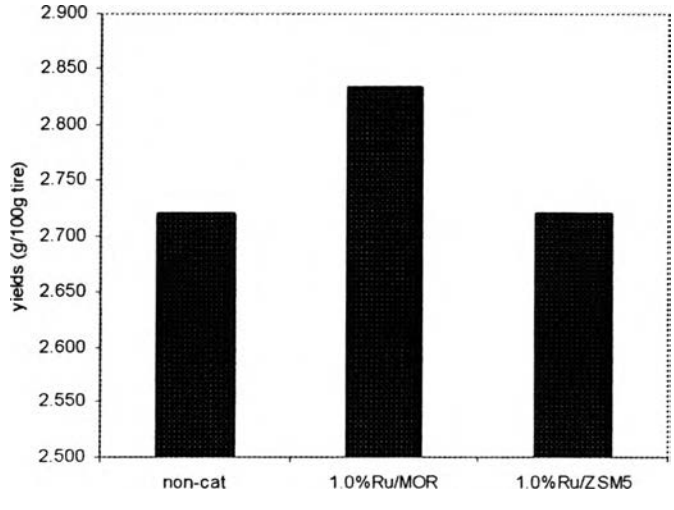


**Figure 4.22** Total light olefin production obtained from different catalysts.

4.2.4 Quality of Pyrolysis Oil

In Figure 4.23, the chemical compositions of pyrolysis oil are classified into saturated hydrocarbons and total aromatic hydrocarbons. The results show that Ru/ZSM5 exhibits the higher amount of aromatic hydrocarbons than Ru/MOR. According to the fact that HZSM5 is well known to have high selectivity for the transformation of n-alkanes due to the steric effect and for the aromatization process (Vasil *et al.*, 1998). So, it might be possible that Ru/ZSM5 accelerates aromatization reaction as compared to olefin formation. That is why the yields to light olefins produced by Ru/ZSM5 are lower than those obtained from Ru/MOR as reported above. On the other hand, aromatic hydrocarbons could be formed by the aromatization reaction of olefins. Ding *et al.* (2007) suggested the series of aromatization reactions of olefins by the role of different types of acid sites. The aromatization of olefins is initiated from the formation of $C_6$-$C_{10}$ olefins via oligomerization of $C_2$-$C_5$ olefins catalyzed by Brönsted acid sites. Then, diolefins were formed via dehydrogenation or hydrogen transfer reactions catalyzed by stronger Lewis or Brönsted acid sites. Next, the cyclization of diolefins was catalyzed by Brönsted acid site to form cycloolefins which finally yield aromatics hydrocarbon via dehydrogenation and hydrogen transfer reaction catalyzed by Lewis and Brönsted acid sites, respectively. Moerover, using Ru/MOR produces the lower amount of asphaltene than Ru/ZSM5 as shown in Figure 4.24.

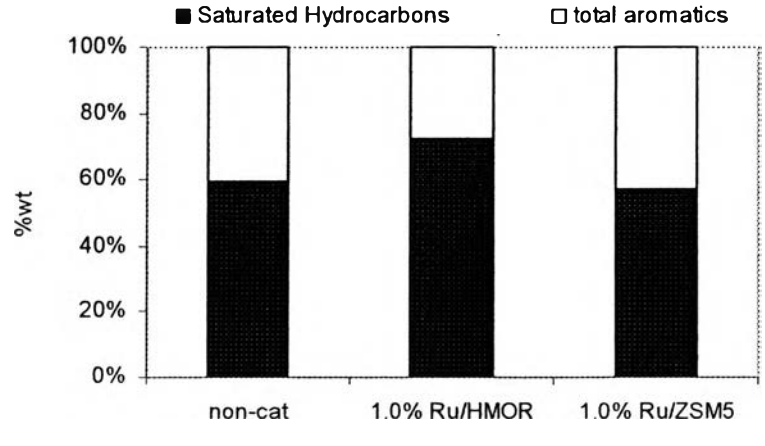


**Figure 4.23** Chemical compositions in oil obtained from different catalysts.

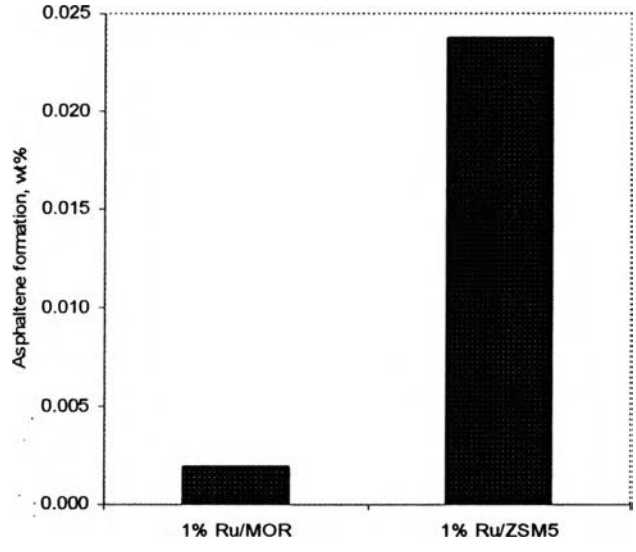


* 0.2% for non-catalytic case

**Figure 4.24** Asphaltene formation from different catalysts.

## 4.3 Effect of Ru Loading Amount

The various amounts of ruthenium was loaded on the HMOR zeolite. The effects of bifunctional catalysts on the pyrolysis products were investigated and discussed as follows..

### 4.3.1 Product Distributions

Figure 4.25 shows the amount of gas and liquid produced by catalytic pyrolysis as compared to non-catalytic pyrolysis. It can be investigated that the gas to liquid ratio of catalytic cases are about 2 times higher than non-catalytic case at the same conditions. This means that the amount of gas produced by the bifunctional catalysts is higher than pyrolysis without catalysts because the higher reaction activity of the catalyst cracked the larger molecules to lower product in the form of incondensable-gaseous products. Otherwise, ruthenium loaded on the zeolite can increase thermal cracking activity.

For the different amounts of metal loaded on the zeolite, it was found that the yield to gas increases with the increasing amount of ruthenium reaching the maximum at 0.7% loading, and then decreases at 1.0 and 1.2% loading. This can be

suggested that too much loading amount suppresses the reaction activity resulting in the lower amount of gaseous product than low metal loading.

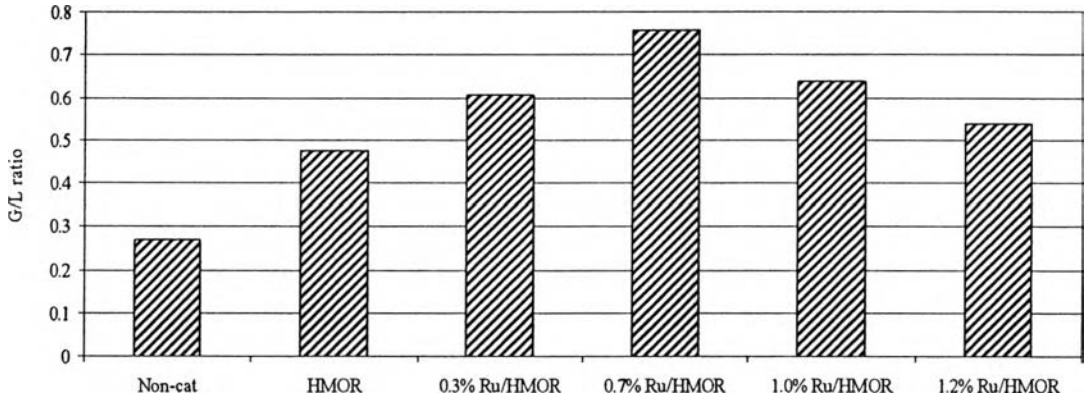


**Figure 4.25** Gas to liquid ratio of bifunctional catalysts.

The solid yields for both catalytic and non-catalytic cases remain constant at about 47.5 %wt by average because the tire is completely cracked into pyrolysis products in the pyrolysis zone at the same condition and no further cracking of solid product is occurred at the catalytic zone. The results are shown in Appendix B.

4.3.2 Gas Composition

The pyrolysis gas is comprised of methane, ethane, ethylene, propane, propylene, mixed-$C_4$, mixed-$C_5$, mixed-$C_6$, mixed-$C_7$, and mixed-$C_8$ hydrocarbons as shown in Figure 4.26. With the addition of catalysts, propane increases about 2 times higher than non-catalytic case when the amount of ruthenium increases to the maximum at 0.7% loading whereas ethylene and propylene decrease with increasing metal loading as compared with non-catalytic case. At 1.2% loading, the compositions of light hydrocarbon gases decrease, consequently increasing the heavy hydrocarbon gases such as, mixed-$C_5$ to mixed-$C_8$. This is possible that too high metal loading causes the decrease in cracking activity of catalyst, so the yields to lower molecular weight products are decreased at high metal loading.

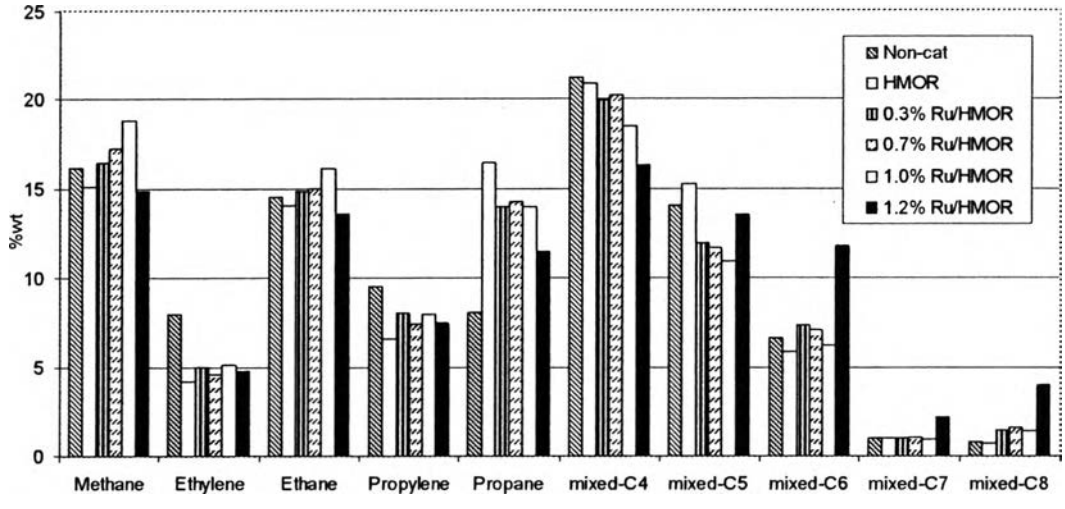


**Figure 4.26** Gas compositions for catalytic pyrolysis.

The percentage of metal loading influencing on the gas composition obtained from catalytic pyrolysis can be observed from Figure 4.27. The amount of metal loading has a greater influence on the gas distribution than on the yields to gas components. When using the zeolite alone, the selectivity to propane increases about twice as much as obtained from non-catalytic case. As ruthenium loading is increasing, the yield to propane decreases subsequently increasing the light olefins yields. The increase in the amounts of $C_2$-$C_3$ compounds and also to methane was reported by Shiraga *et al.* (2007), who studied on the partial oxidation of propane. They found that, in the presence of ruthenium metal, side reactions such as the dehydrogenation of propane, propane cracking, and coke formation could be occurred. These side reactions depending on reactant composition, temperature, residence time, and catalytic system become involved. They suggested that ruthenium metal catalyzed the cracking of propane resulting in high selectivity to methane and $C_2$-$C_3$ compounds. That is why the yields to methane, ethylene and propylene are increased when ruthenium metal is loaded.

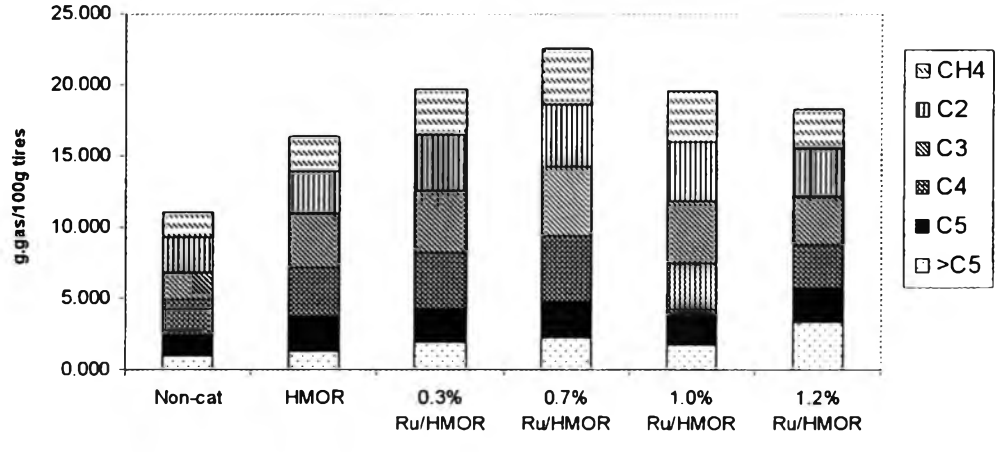


**Figure 4.27** Yields to gas component for different percentages of metal loading.

4.3.3 Light Olefins Production

The variation of the yields to light olefins with the percentage of metal loading is shown in Figure 4.28. Propylene yield is higher than the yield of ethylene for all catalytic cases. The yield of propylene passes through the maxima at 0.7% loading and then decreases as the amount of metal loading increases. Ethylene yield varies slightly at the low percentages of loading, and then decreases at 1.2% metal loading. Similar results were found by Sha *et al.* (1999) and Basu and Kunzru (1992).

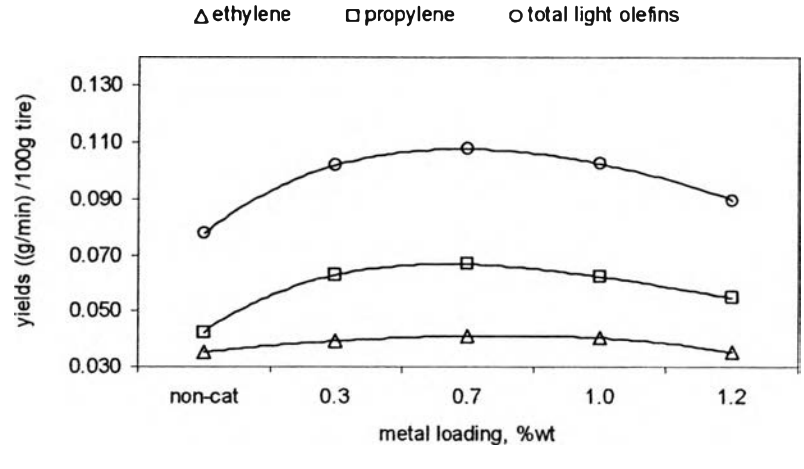


**Figure 4.28** Yields to light olefins for different percentages of metal loading.

Li *et al.* (2005) also concluded that short residence time was suitable for high total light olefins yields, and it was hard to increase light olefins yields by increasing residence time. Also, to the effect of amount of metal loading, the yields to both components varied slightly as the metal loading increased.

### 4.3.4 Liquid Analysis

The quantity and quality of petroleum fraction in pyrolysis oil with different weight percentages of metal loading on HMOR are shown in Figures 4.29-4.30. The boiling point distributions of hydrocarbons in oils were obtained from simulated distillation curves according to ASTM standard method (ASTM D2887, 1989). The main compositions of both catalytic and non-catalytic pyrolysis are gasoline, kerosene, gas oil, and vacuum gas oils.

#### *4.3.4.1 Petroleum Fraction Analysis*

As compared with non-catalytic pyrolysis, the yields to heavy fractions such as light vacuum gas oil and heavy vacuum gas oil drastically decrease with using the catalysts as a result of the increases in the yields to gasoline and kerosene. This can be described that the catalytic cracking reaction occurred so that the chains of heavy molecules break down to lower molecular weight products. In addition, the oils products from both non-catalytic and catalytic pyrolysis are distributed in the ranges of $C_5$ to $C_{50}$. The carbon number distribution of maltenes obtained from catalytic pyrolysis shows the higher yields of gasoline and kerosene while the lower amount of heavy fractions are produced as shown in Figure 4.30. The catalytic pyrolysis can narrow the carbon distribution of pyrolysis oil as compared with non-catalytic pyrolysis. This means that Ru/MOR has very high cracking activity, which is also related to the high yields of gas products as compared with non-catalytic cases as demonstrated above. Similar to Hwang *et al.* (1998), they studied the catalytic degradation of polymer, and found that the carbon distribution of thermal degradation products was distributed in wider ranges than catalytic degradation. Ding *et al.* (1997) also found that the products obtained from the thermal degradation of polyethylene had the carbon number distribution of $C_1$-$C_{27}$

and above, whereas the catalytic cracking of polyethylene gave the narrow range of distribution of $C_1$-$C_{17}$.

For the effects of amount of metal loading on the quantity of petroleum fractions, at a low amount of ruthenium loading, the yield to gas oil is decreased whereas the yields to gasoline and kerosene fractions are increased as shown in Figure 4.29. As the amount of metal loading increases, the yield to kerosene is decreased, consequently increasing in the gas oil yield. The other fractions are slightly changed with the amount of metal loading. Moreover, HMOR gave the highest yield of gasoline and the lowest yields of vacuum gas oils. This can be suggested that the zeolite alone has higher cracking activity than using as a bifunctional catalyst. On the other hand, the zeolite alone has higher acidity than zeolite loaded with noble metal. 0.7% loading shows the maximum yield to kerosene fraction whereas this fraction is started to decrease at 1.0% loading and reaches the minimum at 1.2% loading. In contrary, the gas oil fraction passes through the minimum at 0.7% loading, and reaches maximum at 1.2% loading. This is possible that at high metal loading, partial pore-blocking occurs, so that the acidity of external surface of catalyst is decreased resulting in the lower yield to kerosene fraction when compared with low loading or the zeolite alone. These can also be explained by the BET and TEM results in Table 4.6 and Figure 4.34.

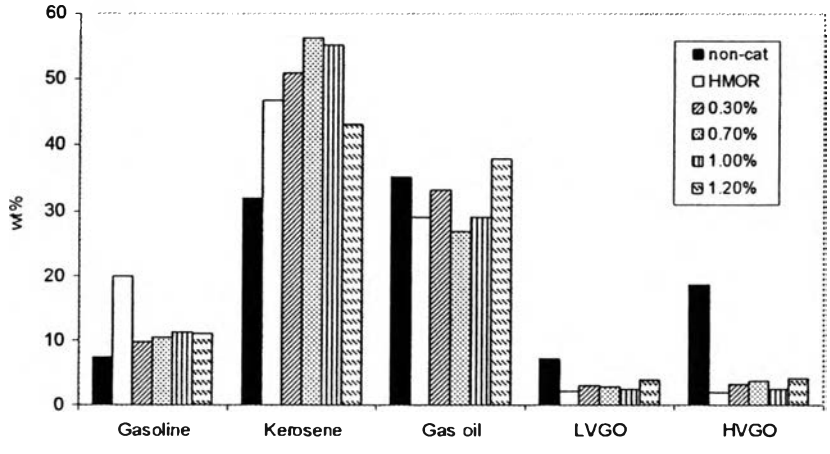


**Figure 4.29** Petroleum fractions in maltenes obtained from non-catalytic and catalytic pyrolysis.

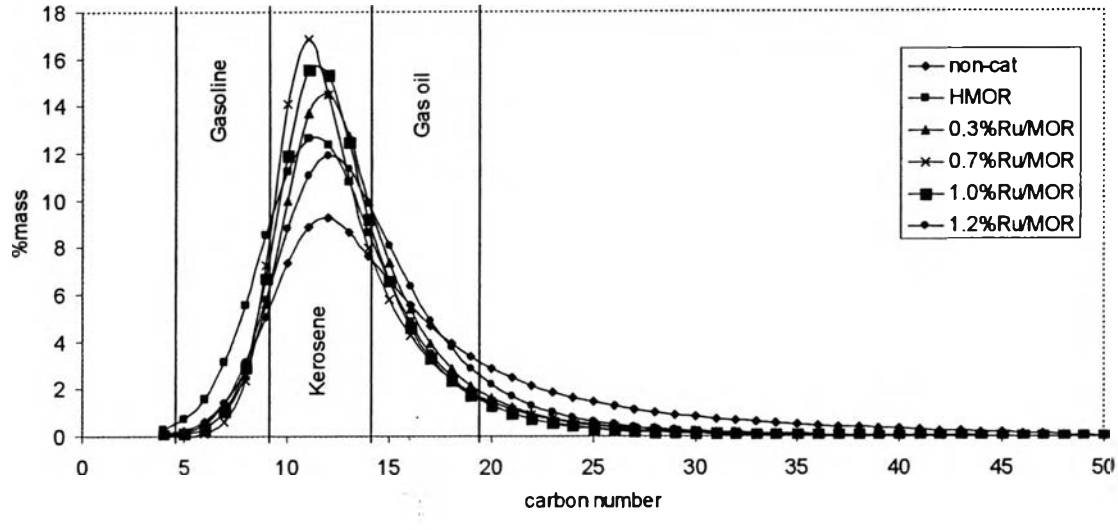


**Figure 4.30** Carbon number distribution of maltene for non-catalytic and catalytic pyrolysis.

*4.3.4.2 Quality of Pyrolysis Oil*

The quality of pyrolysis oil can be roughly estimated by the amount of chemical compositions in the oil such as, saturated hydrocarbons, mono-aromatics, di-aromatics, poly-aromatics and polar-aromatics in the maltene fractions. The ratio of saturated hydrocarbons and total aromatic hydrocarbons are shown in Figure 4.31. It was found that these ratios are comparable for both cases. The increase in the amount of metal causes a slight increase in saturated hydrocarbons, which then decreases as the amount of metal increases. More details on the compositions in aromatic hydrocarbons were investigated and shown in Figure 4.32.

From Figure 4.32, the yield to polar aromatic hydrocarbon decreases whereas the yields to single ring aromatic and poly aromatic hydrocarbons are increased with the increasing of amount of ruthenium loading. Moreover, from the previous section, the yields to light olefins decreased with the increasing amount of metal loading. It is possible that the light olefins molecules combine to form mono-aromatic and poly-aromatic hydrocarbons via the aromatization reaction as reported in the previous section.

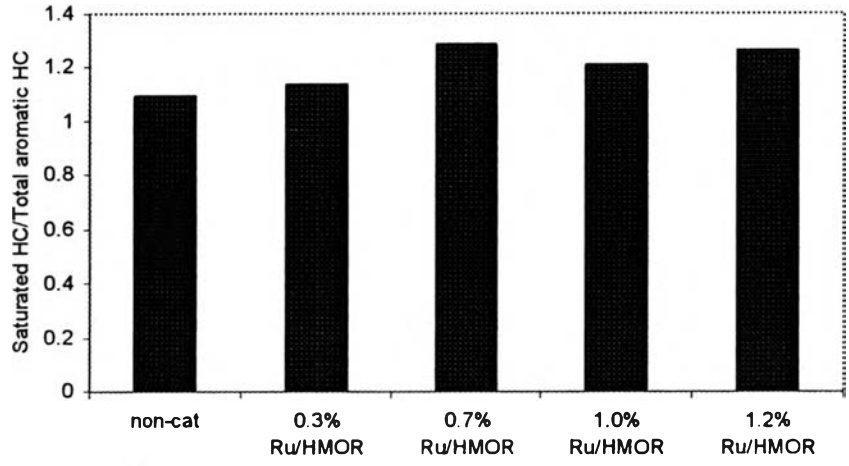


**Figure 4.31** The ratio of saturated hydrocarbons to total aromatic hydrocarbons in maltene obtained from non-catalytic and catalytic pyrolysis.

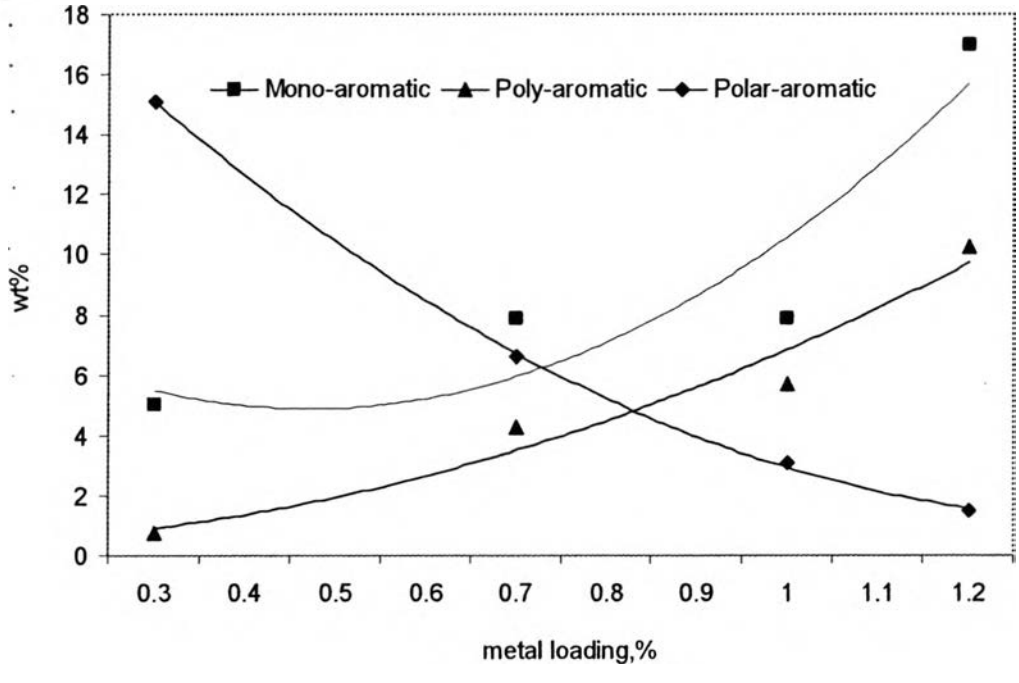


**Figure 4.32** Chemical compositions in maltene for different amounts of metal loading.

Asphaltene reduction in oil products is one criterion to determine which catalyst is better. It was measured from the weight of asphaltene retained on the filter paper after mixing the pyrolyzed oils with n-pentane. The asphaltene can be deposited on the pyrolysis equipment, which can cause problems to the whole process. Therefore, it is more economical to use bifunctional catalysts, which can reduce the amount of asphaltene in oil products.

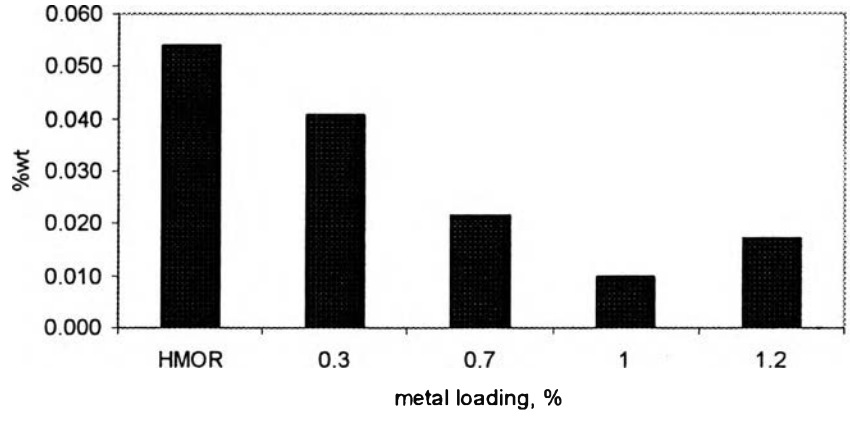


**Figure 4.33** Asphaltene reductions at different residence time and metal loading.

Figure 4.33 shows the reduction of asphaltene with different amounts of ruthenium loaded on mordenite. It can be observed that the amount of asphaltene decreases with the increasing amount of metal loading as compared with non-catalytic case. In addition, 1.0% ruthenium loading exhibits the highest asphaltene reduction in the experiments.

From the results in this part, it is possible that mono-aromatic and poly-aromatic hydrocarbons are formed directly from the cracked molecules of polar-aromatic hydrocarbons. It is also possible that the light olefins molecules are combined to form single ring aromatics, and the single ring aromatics can also combine with another molecules to form bigger molecules such as, PAHs. On the other hand, the single ring and poly-aromatic hydrocarbons might be possibly formed directly from the cracked molecules of asphaltene, which decreased with the increase of metal loading (Douda *et al.*, 2004).

For the role of ruthenium metal on the pyrolysis product, the low amount of ruthenium loading on the zeolite causes the reaction favor on dehydrogenation reaction resulting in the low amount of paraffins molecule and the increase in light olefins. As the metal contents increases, the hydrogen transfer reaction is dominated resulting in the high amount of paraffins and aromatic hydrocarbons (Betancourt *et al.*, 1998). In addition, from the results that polar-aromatic hydrocarbons decrease as the amount of ruthenium metal increases, it might be possible that ruthenium metal strongly reacts with sulphur compounds in polar-aromatic molecules resulting in the dissociation of sulphur molecule from polar compounds. Moreover, the ruthenium metal might prevent the formation of polar compounds as reported to have the highest activity for hydrodesulphurization process (Raje *et al.*, 1997).

Figure 4.34 shows the example reaction of the role of ruthenium on the dissociation of sulphur molecule in polar compounds. As the sulphur molecule was removed, the result molecule can be cracked or reacted further to form small aromatic or poly-aromatic compounds, respectively.

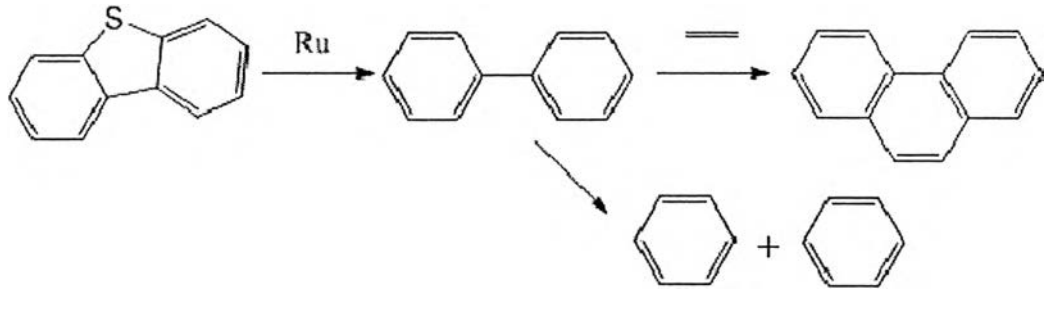


**Figure 4.34** Example reaction of mono-aromatic and poly-aromatic formation from polar-aromatic molecule (Ekinci *et al.*, 2002).

## 4.4 Catalyst Characterization

### 4.4.1 Crystal Structure of Catalysts

XRD patterns of bifunctional catalysts are shown in Figure. 4.35. It can be observed that every bifunctional catalysts present standard X-ray diffraction

patterns according with the topology of mordenite and that the process of ruthenium metal impregnation, and calcinations did not affect the zeolitic structure. The signal for metallic ruthenium was found with a small intensity at $2\theta = 44°$. In addition, no evidence for the ruthenium oxide peak in the prepared catalyst is observed.

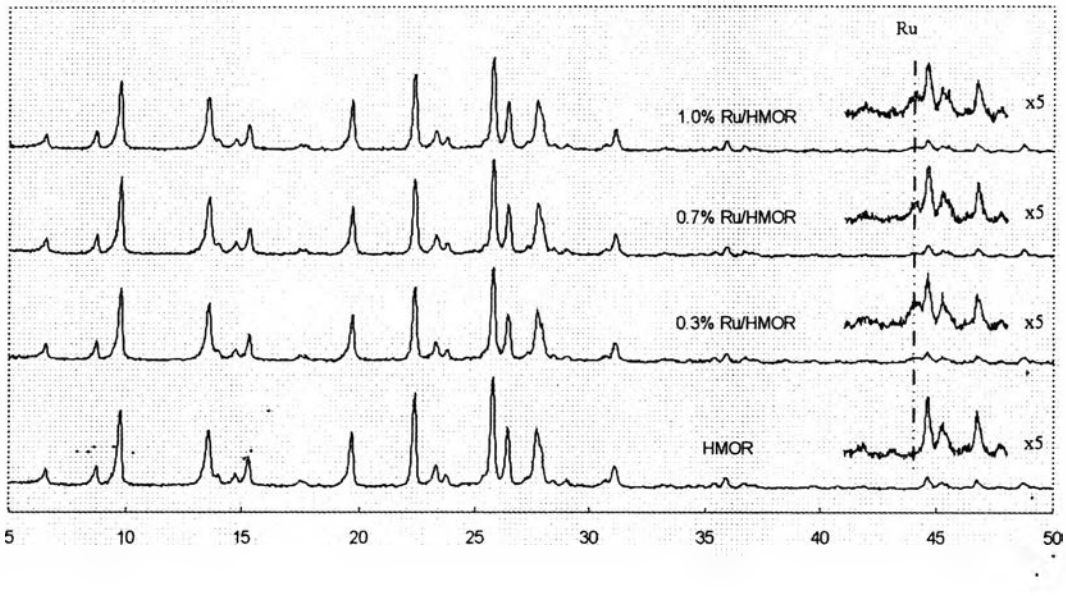


**Figure 4.35** The XRD patterns of HMOR and Ru/HMOR with different amounts of loading.

4.4.2 Metal Particle Size

The incipient wetness impregnation method provided the metal particle size in the ranges of 5 to 20 nm. Moreover, most of the ruthenium particles are well dispersed and located at the outer surface of the zeolite. These results are similar to XRD patterns which small size of ruthenium metals is observed. At the high amount of metal loading, some of metal particles are accumulated on the surface of zeolite, and block the pore of the zeolite which might be resulted in the low cracking activity of the catalysts.

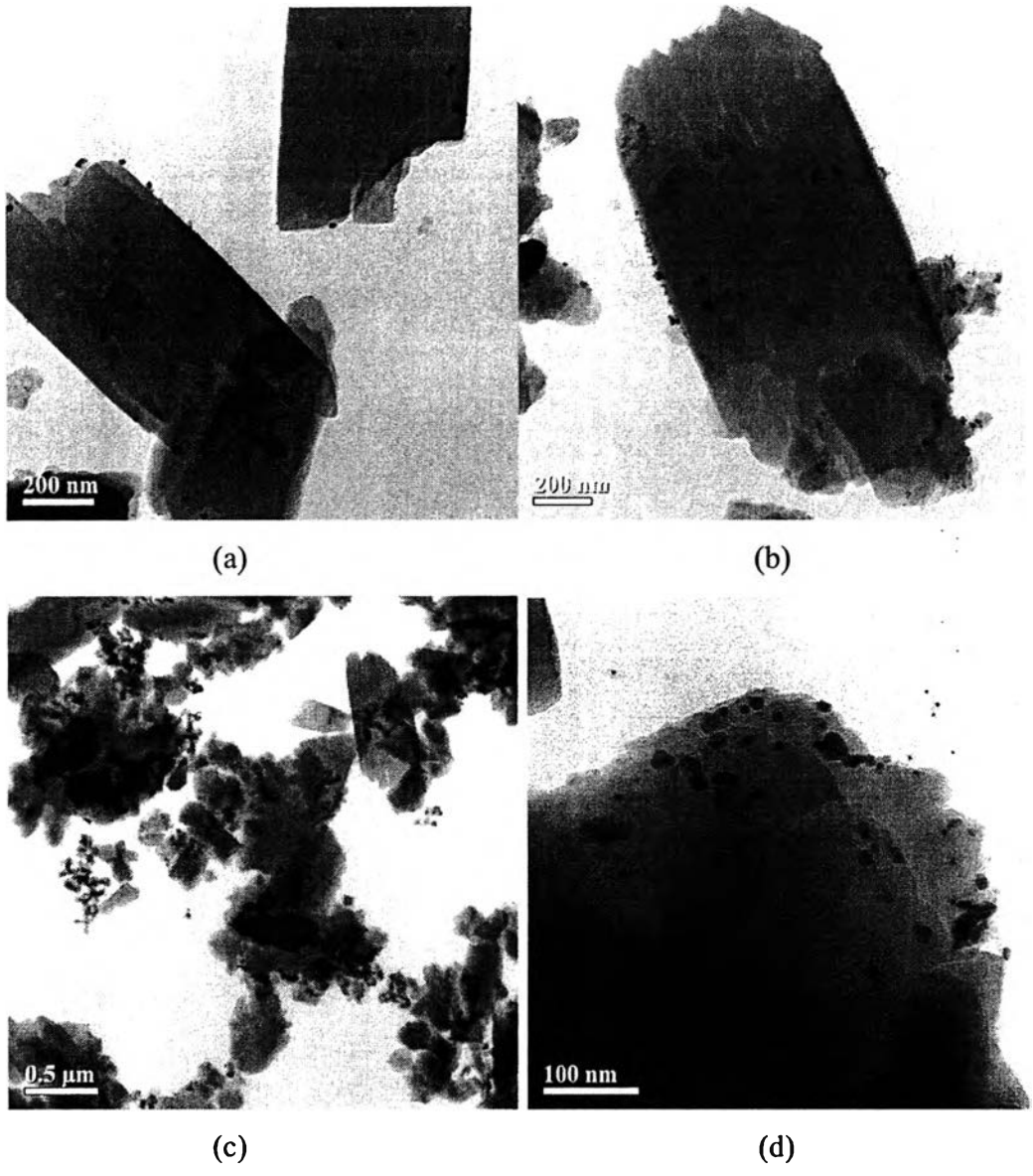


**Figure 4.36** The TEM images of of Ru/MOR : (a) 0.3% Ru/MOR, (b) 0.7% Ru/MOR, (c) 1.0% Ru/MOR, and (d) 1.2% Ru/MOR.

4.4.3 Specific Surface Area

The surface area of catalysts was measured by using BET method. As the ruthenium metal amount increases, the surface area of catalyst is slightly decreased. Moreover, the surface area of catalyst is significantly decreased at 1.2% loading. This can confirm the results of partial pore blocking of zeolite by the agglomeration of ruthenium metal on the catalysts.

**Table 4.6** BET surface area of Ru-loaded mordenite zeolites with various percentages of Ru

| Catalyst | %Ru | Surface area ($m^2/g$) |
|---|---|---|
| Mordenite | - | 462.1 |
| | 0.3 | 449.9 |
| | 0.7 | 437.2 |
| | 1.0 | 432.7 |
| | 1.2 | 369.9 |